The Journal of Experimental Medicine

Critical Roles of Pten in B Cell Homeostasis and Immunoglobulin Class Switch Recombination

Akira Suzuki,[1, 3, 8] Tsuneyasu Kaisho,[2, 4] Minako Ohishi,[1] Manae Tsukio-Yamaguchi,[1] Takeshi Tsubata,[5] Pandelakis A. Koni,[7] Takehiko Sasaki,[6, 8] Tak Wah Mak,[8] and Toru Nakano[1]

[1]*Department of Molecular Cell Biology, and* [2]*Department of Host Defense, Research Institute for Microbial Disease, Osaka University, Osaka 565-0871, Japan*

[3]*Department of Biochemistry, Akita University School of Medicine, Akita 010-8543, Japan*

[4]*RIKEN Research Center for Allergy and Immunology, Kanagawa 230-0045, Japan*

[5]*Department of Immunology, Medical Research Institute, Tokyo Medical and Dental University, Tokyo 113-8510, Japan*

[6]*Department of Pharmacology, Tokyo Metropolitan Institute of Medical Science, Tokyo 113-8613, Japan*

[7]*Molecular Immunology Program, Institute of Molecular Medicine and Genetics, Medical College of Georgia, Augusta, GA 30912*

[8]*Advanced Medical Discovery Institute and Department of Medical Biophysics, University of Toronto, Toronto, Ontario M5G 2C1, Canada*

Abstract

Pten is a tumor suppressor gene mutated in human cancers. We used the Cre-loxP system to generate a B cell–specific mutation of Pten in mice (*bPten*$^{flox/flox}$mice). *bPten*$^{flox/flox}$ mice showed elevated numbers of B1a cells and increased serum autoantibodies. Among B2 cells in *bPten*$^{flox/flox}$ spleens, numbers of marginal zone B (MZB) cells were significantly increased while those of follicular B (FOB) cells were correspondingly decreased. Pten-deficient B cells hyperproliferated, were resistant to apoptotic stimuli, and showed enhanced migration. The survival kinase PKB/Akt was highly activated in Pten-deficient splenic B cells. In addition, immunoglobulin class switch recombination was defective and induction of activation-induced cytidine deaminase (AID) was impaired. Thus, Pten plays a role in developmental fate determination of B cells and is an indispensable regulator of B cell homeostasis.

Key words: PTEN • mutation • marginal zone B cells • class switch recombination • activation-induced cytidine deaminase

Introduction

PTEN is a tumor suppressor gene mutated in many human sporadic cancers (1) and in hereditary cancer syndromes such as Cowden disease and Bannayan-Zonana syndrome (2, 3). Functionally, PTEN is a dual protein and lipid phosphatase (4, 5). The major substrate of PTEN is phosphatidyl inositol-3,4,5-triphosphate (PIP3),* a second messenger molecule produced through PI3′K activation induced by growth factor stimulation. PIP3 activates the serine-threonine kinase PKB/Akt which is involved in anti-apoptosis, proliferation, and oncogenesis. PTEN negatively regulates cell survival by dephosphorylating PIP3.

In previous work, we showed that a null mutation of Pten in mice (*Pten*$^{-/-}$ mice; reference 6) is embryonic lethal. Using *Pten*$^{-/-}$ mouse embryonic fibroblasts (MEFs), we demonstrated that PKB/Akt is hyperactivated in the absence of Pten (7). Furthermore, *Pten*$^{+/-}$ mice frequently develop lymphoid hyperplasia, T cell lymphomas, and endometrial, prostatic, and breast cancers (6, 8, 9). Autoimmune disorders are also prevalent in *Pten*$^{+/-}$ mice (10). In T cell–specific Pten-deficient mice, we showed that CD4^{+} lymphomas and autoimmune disorders arise due to impaired thymic negative selection and peripheral tolerance (11). Since Pten mutations occur in human B cell malignancies (12–14), we investigated the role of Pten in B

T. Kaisho, M. Ohishi, and M. Tsukio-Yamaguchi contributed equally to this work.

Address correspondence to Tak Wah Mak, Advanced Medical Discovery Institute, 620 University Ave., Toronto, Ontario M5G 2C1, Canada. Phone: 416-204-5302; Fax: 416-204-5300; E-mail: tmak@uhnres.utoronto.ca

A. Suzuki's present address is Department of Biochemistry, Akita University School of Medicine, Akita 010-8543, Japan.

**Abbreviations used in this paper:* BM, bone marrow; CSR, class switch recombination; DC, digestion-circulation; FOB, follicular B; MEF, mouse embryonic fibroblast; MLN, mesenteric lymph node; MZB, marginal zone B; PEC, peritoneal cavity; PIP3, phosphatidyl inositol-3,4,5-triphosphate; SDF, stromal cell–derived factor; TD, thymus-dependent; TI, thymus-independent antigen.

 J. Exp. Med. © The Rockefeller University Press • 0022-1007/2003/03/657/11 $8.00
Volume 197, Number 5, March 3, 2003 657–667
http://www.jem.org/cgi/doi/10.1084/jem.20021101

cell development and B cell–associated autoimmunity and oncogenesis.

B cells can be classified as either B1 or B2 cells. B1 cells occur mainly in the pleural and peritoneal cavities and are associated with the production of autoreactive antibodies (15). B2 cells are found chiefly in the periphery and comprise transitional T1 and T2 cells, and mature follicular B (FOB) cells and marginal zone B (MZB) cells. FOB cells form the follicular structures of the secondary lymphoid organs and are capable of recirculation. The much smaller MZB fraction resides in the spleen at the boundary between the red pulp and white pulp (16). These cells may be the first splenocytes to encounter blood-borne bacterial pathogens (16, 17). Splenic MZB cells, but not FOB cells, have high levels of surface immunoglobulin M (IgM) and the complement receptor CD21, and low levels of IgD and CD23 (18, 19). Both MZB and FOB cells undergo immunoglobulin class switching in response to antigen stimulation and cytokines (20). Class switch recombination (CSR) requires the activity of the RNA editing enzyme AID (21) but the underlying mechanism is unknown.

To investigate the role of Pten in B cells, we generated *bPten*$^{flox/flox}$ mice using the Cre-loxP system. We report that Pten governs B cell subsets especially in B1, FOB, and MZB cells and is required for normal immunoglobulin class switching.

Materials and Methods

Generation of bPten$^{flox/flox}$ *Mice.* *Pten*$^{flox/flox}$ mice (C57BL6/J background) were mated to *CD19Cre* transgenic mice (C57BL6/J background; reference 22) in which expression of Cre is controlled by the endogenous promoter of the B cell–specific gene CD19. Offspring carrying *CD19Cre* and two copies of the floxed *Pten* allele (CD19CrePten$^{flox/flox}$), *CD19Cre* plus one copy of the floxed *Pten* allele (CD19CrePten$^{flox/+}$), and *CD19Cre* plus two copies of the WT *Pten* allele (CD19CrePten$^{+/+}$) were used in the analyses as homozygous mutant (*bPten*$^{flox/flox}$), heterozygous mutant (*bPten*$^{flox/+}$), and wild type (*bPten*$^{+/+}$) mice, respectively.

PCR Analysis of Pten Genotypes. Genomic DNA from mouse tails was isolated and amplified by PCR following a published protocol (6). Sense primer (5′-GTCACCAGGATGCTTCT-GAC-3′) and antisense primer (5′-GAAACGGCCTTAAC-GACGTAG-3′) were used to detect the floxed *Pten* allele; sense primer (5′-GTCACCAGGATGCTTCTGAC-3′) and antisense primer (5′-GTGACATCAACATGCAACACTG-3′) were used to detect the WT *Pten* allele; and sense primer (5′-CTCCT-CACCTGTCTCTTCTG-3′) and antisense primer (5′-TTC-CATGAGTGAACGAACCTGGTCG-3′) were used to detect the *CD19Cre* transgene. Amplified fragments of 512, 413, and about 500 bp, respectively, were obtained.

Southern and Western Blots. Genomic Southern blots were performed using a previously described probe and protocol (6). For Western blots, B cells (2×10^6) were either left untreated or stimulated with 10 μg/ml anti-IgM (ICN Biomedicals/Cappel). Total cell lysates were prepared and 10 μg lysate aliquots analyzed by Western blotting as described (7). Antibody directed against the NH_2 terminus of Pten and anti-actin antibody were from Santa Cruz Biotechnology, Inc.; anti-phospho-PKB/Akt (Ser473) and anti-total Akt/PKB antibodies were from New England Biolabs, Inc. For PI3′K inhibition studies, an optimal amount of wortmannin (200 nM; Sigma-Aldrich) or LY294002 (50 μM; Sigma-Aldrich) as determined in pilot studies was added 15 min before stimulation.

Flow Cytometric Analysis and Cell Purification. Single cell suspensions were first incubated with anti-CD16/32 to minimize nonspecific staining. Cells were then stained with cocktails of various mAbs conjugated to FITC, PE, or biotin for 20 min at 4°C. Biotinylated mAbs were developed with streptavidin-Cy-Chrome (BD Biosciences). All mAbs, except PE-labeled anti-IgD (Southern Biotechnology Associates, Inc.), were purchased from BD Biosciences. Flow cytometric analysis was performed using a FACSCalibur™ (Becton Dickinson) with CELLQuest™ software (Becton Dickinson). Total splenic B cells were purified using B220 magnetic beads (Macs; Miltenyi Biotec). Splenic CD23^{high}CD21^{low} B cells and CD23^{low}CD21^{high} B cells were purified using B220 magnetic beads followed by cell sorting with a FACSVantage™ (Becton Dickinson) after staining with anti-CD21/35-FITC and anti-CD23-PE antibodies (BD Biosciences).

Histological Analysis of Splenic Sections. For immunohistochemical staining, freshly dissected spleens were covered with Tissue-Tek OCT compound (Miles, Inc.) and quickly frozen in liquid nitrogen. Frozen sections (7-μm thick) were fixed in ice cold acetone and incubated in 3% H_2O_2 in 50% methanol for 30 min to inactivate internal peroxidase. Immunofluorescent staining was performed using MOMA-1 (Serotec) and anti–rat Alexa488 (Molecular Probes) antibodies followed by anti-B220-PE (BD Biosciences) staining. Immunohistochemical staining was performed using biotin-conjugated peanut agglutinin (PNA; Seikagaku Kogyo) followed by a Vectastain ABC Elite kit (Vector Laboratories).

Analysis of Humoral Responses. Serum Ig isotype concentrations were analyzed by ELISA as described (23). Abs and standard Igs were purchased from Southern Biotechnology Associates, Inc. For T cell–dependent immune responses, mice were immunized with 100 μg of alum-precipitated chicken γ-globulin (CG) coupled to 4-hydroxy-3-nitro-phenylacetyl (NP). For T cell–independent immune responses, mice were immunized with 100 μg of alum-precipitated Ficoll coupled to NP. In both cases, mice were bled at 7 and 14 d after challenge. Serum titers of NP-specific IgM, IgG1, and IgG3 were determined by ELISA as described (23). The measurement of serum anti-ssDNA IgG and IgM antibodies was performed using ELISA as described (24). Statistical analyses were performed using the unpaired Student's *t* test.

Lymphocyte Activation in Culture. Splenic B cells were purified using B220 microbeads and a Magnetic Cell Sorter (MACS; Miltenyi Biotec). B cells (2×10^5/well) were stimulated for 4 d with 50 μg/ml LPS alone or 50 μg/ml LPS plus 800 U/ml IL-4 in RPMI 1640 medium supplemented with 20% FCS, 2-mercaptoethanol (ME), penicillin, and streptomycin. Cells and culture supernatants were analyzed by flow cytometry and ELISA, respectively.

RT-PCR. Cells (5×10^5/ml) were stimulated in vitro for 2 d with 50 μg/ml LPS alone or LPS plus 800 U/ml of IL-4. Total RNA was extracted using TRIzol (GIBCO BRL) according to the manufacturer's instructions. For PCR of germline transcripts, the following standard primers were used to obtain the indicated sizes of products: (μ) ImF and CmR, 245 bp; (γ3) Ig3F and Cg3R, 323 bp; (γ1) Ig1 and Cg1R, 429 bp. Post-switch transcripts were amplified using the following primer pairs: (γ3) ImF and Cg3R, 323 bp; (γ1) ImF and Cg1R, 353 bp. Germline and post-switch transcripts were amplified using 30 cycles of PCR. The primer sequences were as follows: ImF; 5′-CTCTGGC-CCTGCTTATTGTTG-3′, CmR: 5′-GAAGACATTTGG-

GAAGGACTGACT-3′, Ig3F: 5′-TGGGCAAGTGGATCT-GAACA-3′, Cg3R: 5′-CTCAGGGAAGTAGCCTTTGACA-3′, Ig1: 5′-GGCCCTTCCAGATCTTTGAG-3′, Cg1R: 5′-GGATCCAGAGTTCCAGGTCACT-3′.

For amplification of the AID transcript, the primer pair of 5′-GAGGGAGTCAAGAAAGTCACGCTGGA-3′ and 5′-GG-CTGAGGTTAGGGTTCCATCTCAG-3′ was used in 30 cycles of PCR. For amplification of MSH2 transcripts, the primers 5′-CTAAGGAGACGCTGCAGTTG-3′ and 5′-TACTGGC-GAACCAGAAGAAG-3′ were used. For amplification of the HPRT transcript, the primers 5′-GATTAGCGATGATGA-ACCAGG-3′ and 5′-ACAGTAGCTCTTCAGTCTGATA-3′ were used.

Digestion-Circularization-PCR. Digestion-circularization (DC)-PCR analysis was performed as described (25). Briefly, genomic DNA was isolated from B cells cultured in vitro for 4 d with LPS (50 μg/ml) and IL-4 (800 U/ml). After EcoRI digestion, genomic DNA was purified and self-ligated. Ligated DNA was purified and used as a template for PCR using primers as reported previously for μ-γ1 (25).

B Cell Proliferation. Splenic B cells were purified using B220 magnetic beads and $CD23^{low}CD21^{high}$ cells or $CD23^{high}CD21^{low}$ cells were isolated by cell sorting. Purified cells (10^5) were placed into round-bottomed 96-well plates in RPMI 1640 medium containing 10% FCS. Anti-IgM (50 μg/ml; ICN Biomedicals/Cappel), IL-4 (100 ng/ml; PeproTech), anti-CD40 (5 μg/ml; BD Biosciences), LPS (2.5 μg/ml; Sigma-Aldrich) or PDBu (20 ng/ml; Sigma-Aldrich) plus ionomycin (2 μg/ml; Sigma-Aldrich) were added to cultures. Cells were harvested on day 2 after a 12 h pulse with 1μCi [^{3}H]thymidine (Amersham) per well.

Apoptosis of "Small Dense" B Cells. Anti-Ig antibody was immobilized by incubating PBS containing 100 μg/ml $F(ab')_2$ fragments of affinity-purified goat anti–mouse IgM antibody (ICN Biomedicals) in wells of plastic dishes at 37°C overnight, followed by washing with PBS. "Small dense" B cells were prepared by depleting T cells from mouse splenocytes using anti-Thy1.2 F7D5 (Serotec), anti-CD4 RL172.5 (a kind gift of Dr. Kina, Kyoto University, Kyoto, Japan), anti-CD8 3.155 (American Type Culture Collection no.TIB211) and Low-Tox-M rabbit complement (Cedarlane), followed by fractionation using density gradient centrifugation through Percoll (BD Biosciences). Small dense B cells were then cultured in dishes containing immobilized anti-Ig antibody in RPMI 1640 medium supplemented with 10% FCS, 50 μM 2-ME, and 2 mM L-glutamine for up to 24 h. The percentage of viable cells was determined by trypan blue exclusion. Viability results were calculated as a comparison of the percentage of viable cells remaining after treatment relative to the viability of untreated cells cultured for the same length of time.

B Cell Migration Assay. Splenic B cells (10^6) purified using B220 magnetic beads were assayed for transmigration using a 6.5 μm diameter, 3 μm pore size transwell culture dish insert (Costar). Migration was allowed to proceed for 3 h from the top chamber containing RPMI supplemented with 0.25% human serum albumin to the bottom chamber containing 0–300 ng/ml of human stromal cell–derived factor (SDF)-1α (R&D Systems). Cells before and after migration were stained for CD23 and CD21/35 as described above and counted with a FACScan™. The percent change in the populations of each chamber after migration was calculated as (the percent of $CD21^{high}CD23^{low}$ or $CD21^{low}CD23^{high}$ cells in the chamber after migration)/(the percent of these cells in the chamber before migration) × 100%.

Results

Generation of B Cell-specific Pten-deficient Mice. B cell–specific Pten-deficient mice (*bPten*$^{flox/flox}$ mice) were generated by crossing *CD19Cre* transgenic mice (22) to mice homozygous for the floxed Pten allele (*Pten*$^{flox/flox}$ mice; reference 11). *bPten*$^{flox/flox}$ mice were born alive and appeared healthy. Genomic Southern blotting showed that, in the vast majority of mutant B cells, Cre-mediated recombination of *loxP* sites deleted much of the 6.0 kb *Ptenflox* allele, leaving the 2.3 kb *PtenΔ* allele (Fig. 1 A). The deletion of

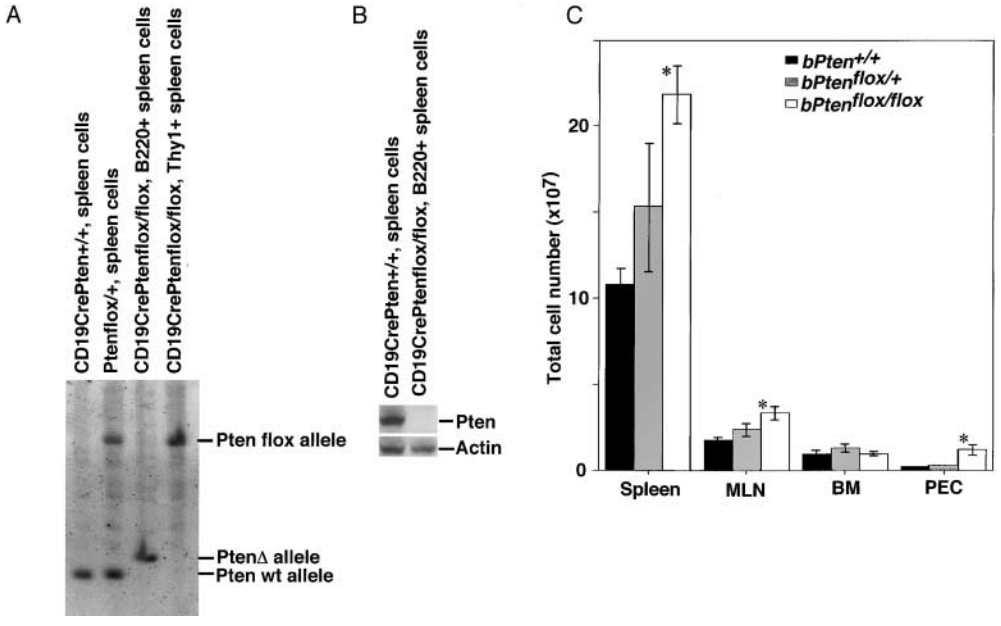

Figure 1. Generation of B cell–specific Pten deficient ($bPten^{flox/flox}$) mice and analysis of enlarged lymphoid organs. (A) Genomic Southern blot. DNA (20 μg) was extracted from the indicated cells, digested with HindIII, and hybridized to a previously described probe (reference 11). The vast majority of B cells from *CD19CrePten*$^{flox/flox}$ mice (*bPten*$^{flox/flox}$ mice) showed a B cell–specific deletion of the Pten gene. (B) Western blot analysis of Pten protein from the indicated cells using Pten antibody and control actin antibody. (C) Splenomegaly, lymph node swelling, and abundant peritoneal cells in *bPten*$^{flox/flox}$ mice. Results shown are the absolute numbers of splenocytes (Spleen), mesenteric lymph node cells (MLN), bone marrow cells (BM), and cells in the PEC from 6–8-wk-old *bPten*$^{+/+}$ ($n = 3$), *bPten*$^{flox/+}$ ($n = 3$), and *bPten*$^{flox/flox}$ ($n = 3$) mice. Where appropriate in all figures, the results are expressed as the mean ± SEM of the indicated number of mice per group. Statistical differences in all cases were determined using the Student's *t* test; *$P < 0.05$.

Pten was confirmed at the protein level by Western blotting using antibody recognizing the NH_2 terminus of Pten (Fig. 1 B). The frequencies of gene deletion observed in $B220^{dull}$ $CD5^+$ peritoneal cavity (PEC) cells and $B220^+$ spleen cells were comparable (unpublished data). The health of 30 *bPten*$^{flox/flox}$ mice and 30 control *CD19 CrePten*$^{+/+}$ *(bPten*$^{+/+}$*)* mice was monitored for over 12 mo. All mutant mice survived the observation period and no tumor formation was observed.

Altered B Cell Populations. *bPten*$^{+/+}$ and *bPten*$^{flox/flox}$ mice were killed at 6–8 wk of age, and B cell subpopulations in the spleen, mesenteric lymph nodes (MLNs), bone marrow (BM), and PEC were examined. Total numbers of splenocytes, MLN cells, and PEC cells in *bPten*$^{flox/flox}$ mice were increased 2.0-fold, 1.9-fold, and 5.5-fold, respectively (Fig. 1 C). Although PTEN is expressed in WT pro-B cells and pre-B cells as well as in mature B2 cells, there were no obvious differences in either the total number of BM cells, or in numbers of pro-B cells ($CD43^+$, $B220^+$, IgM^-) or pre-B cells ($CD43^-$, $B220^+$, IgM^+) in the BM of WT and mutant mice (unpublished data).

The increased B cell number in the PEC was due to a 24-fold increase in $CD5^{dull}B220^{dull}$ cells (Fig. 2 A, top panel; Fig. 2 B, left). These cells expressed Mac-1^{low}, $CD21^-$, $CD23^-$, and HSA^+, compatible with the surface phenotype of B1a cells (unpublished data; references 26 and 27). $CD5^{dull}B220^{dull}$ cells were also increased 11-fold in the spleens of *bPten*$^{flox/flox}$ mice compared with *bPten*$^{+/+}$ spleens (Fig. 2 A, bottom panel; Fig. 2 B).

As shown in Fig. 2 C, IgM^+IgD^- B cells were also elevated in *bPten*$^{flox/flox}$ spleens. Although $CD5^{dull}$ $B220^{dull}$ cells belong to the IgM^+IgD^- population, the increase in their numbers could account for only a part of this elevation. WT splenic IgM^+IgD^- B cells include MZB cells ($CD21^{high}CD23^{low}$), a population that was dramatically increased in *bPten*$^{flox/flox}$ mice (Fig. 2, D, F, and G). FOB cells ($CD21^{low}CD23^{high}$) were decreased not only in relative number (Fig. 2 D), but also in absolute number (Fig. 2 G). Immunohistochemical staining revealed that most of the B2 cells were located in marginal zones, while only a few appeared to be in follicular regions in the *bPten*$^{flox/flox}$ spleen (Fig. 2 E). A similar skewing of cell numbers was noted in *bPten*$^{flox/flox}$ lymph nodes (unpublished data). The percentage of total lymph node B lymphocytes that were $CD21^{high}CD23^{low}$ was 5.2 ± 1.1% in the WT and 31.8 ± 2.9% in the mutant, while the percentage of $CD21^{low}$ $CD23^{high}$ cells was 66.4 ± 2.0% in the WT and 23.94 ± 1.8% in the mutant. In contrast, the absolute numbers of transitional T1 ($IgM^+CD21^{low}CD23^{low}$) and T2 cells ($IgM^+CD21^{high}CD23^{high}$) in the *bPten*$^{flox/flox}$ spleen were increased to the same extent as total B cell numbers (Fig. 2 G), although the relative number of T1 cells in the $CD23^{low}$

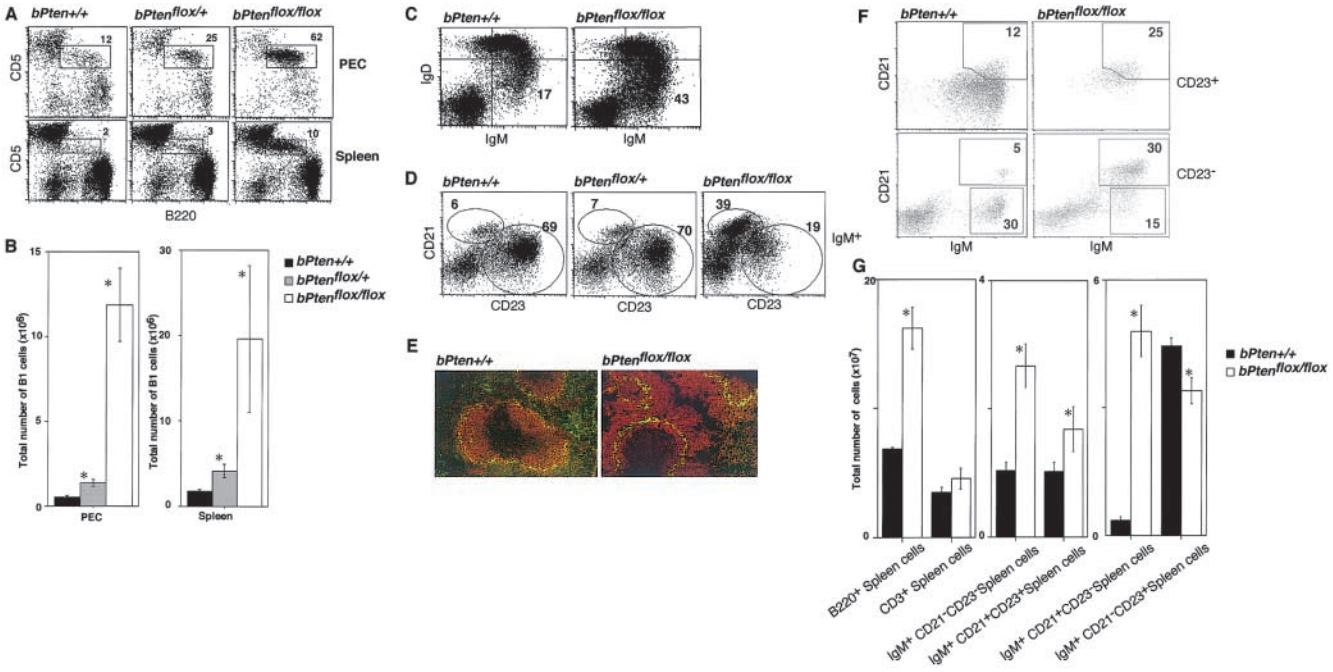

Figure 2. Pten deficiency alters B1a, MZB. and FOB B cell subsets. (A and B) Accumulation of B1a cells in *bPten*$^{flox/flox}$ mice. Increased numbers of $CD5^{dull}B220^{dull}$ cells in the PEC and spleen of 6–8-wk-old *bPten*$^{flox/flox}$ mice were apparent when analyzed by either flow cytometry (A) or total cell counts (B). (C) Increased IgM^+IgD^- cell numbers in the *bPten*$^{flox/flox}$ spleen. Levels of surface IgM and IgD were determined by flow cytometry. (D–F) Alterations to B cell subsets. Flow cytometric (D and F) and total cell count (G) analyses were used to evaluate mature $IgM^+CD21^{high}CD23^{low}$ cells (putative MZB cells; D and F) and $IgM^+CD21^{low}CD23^{high}$ cells (putative FOB cells; D), and transitional $IgM^+CD21^{low}CD23^{low}$ cells (putative T1 cells; F) and $IgM^+CD21^{high}CD23^{high}$ (putative T2 cells; F) among splenic B cells of 6–8-wk-old *bPten*$^{flox/flox}$ and *bPten*$^{+/+}$ mice. Immunohistochemical analysis (E) using MOMA1 (green) and B220 (red) antibodies shows a dramatic increase in MZB cells among B2 cells in *bPten*$^{flox/flox}$ mice, while the number of FOB cells is markedly reduced. For B and E, results are expressed as the mean ± SEM for 6 mice per group. For A, C, D, E, and F, one result representative of seven independent experiments is shown.

population was significantly reduced (Fig. 2 G). The overall segregation of T cell and B cell zones was not impaired in the splenic white pulp, MLN, or Peyer's patches of *bPten*$^{flox/flox}$ mice (unpublished data). Thus, B cell–restricted Pten deficiency results in discrete alterations to the B1a, MZB, and FOB subsets of B lymphocytes.

Impaired Humoral Immunity. To determine whether the altered B cell populations in the mutant mice affected humoral immunity, we assessed serum Ig levels in *bPten*$^{flox/flox}$ mice at 8 weeks of age. As shown in Fig. 3 A, marked decreases in most IgG subclasses and IgA were observed in *bPten*$^{flox/flox}$ mice compared with *bPten*$^{+/+}$ mice. In contrast, serum IgM levels in *bPten*$^{flox/flox}$ mice were elevated fourfold over normal.

We then examined the humoral responses of *bPten*$^{+/+}$ and *bPten*$^{flox/flox}$ mice immunized with either the thymus-dependent (TD) antigen NP-CG (nitro-phenylacetyl-chicken γ-globulin) or the thymus-independent antigen (TI) type II NP-Ficoll. Production of antigen-specific IgG in response to TD antigen was dramatically decreased in *bPten*$^{flox/flox}$ mice (Fig. 3 D) as was germinal center formation (Fig. 3, B and C). Production of antigen-specific IgG in response to TI-II antigen was also severely impaired in the absence of Pten (Fig. 3 E). Thus, an absence of Pten impairs both TD and TI IgG responses.

Reduction of CSR. Because of the altered serum Ig profile observed in *bPten*$^{flox/flox}$ mice, we examined isotype switching in vitro in *bPten*$^{flox/flox}$ B cells. *bPten*$^{+/+}$ and *bPten*$^{flox/flox}$ B cells were cultured for 4 d in the presence of the nonspecific B cell stimulator LPS with or without IL-4. Trypan blue exclusion analysis confirmed that the viability of stimulated cells of both genotypes was not significantly different (unpublished data). Stimulated cells were surface-stained with anti-IgG1 or anti-IgG3 antibody and subjected to flow cytometric analysis. LPS plus IL-4, but not LPS alone, induced switching to IgG1 in WT cells (Fig. 4 A). Prolonged stimulation of WT cells with LPS alone induced switching to IgG3 which was down-regulated by

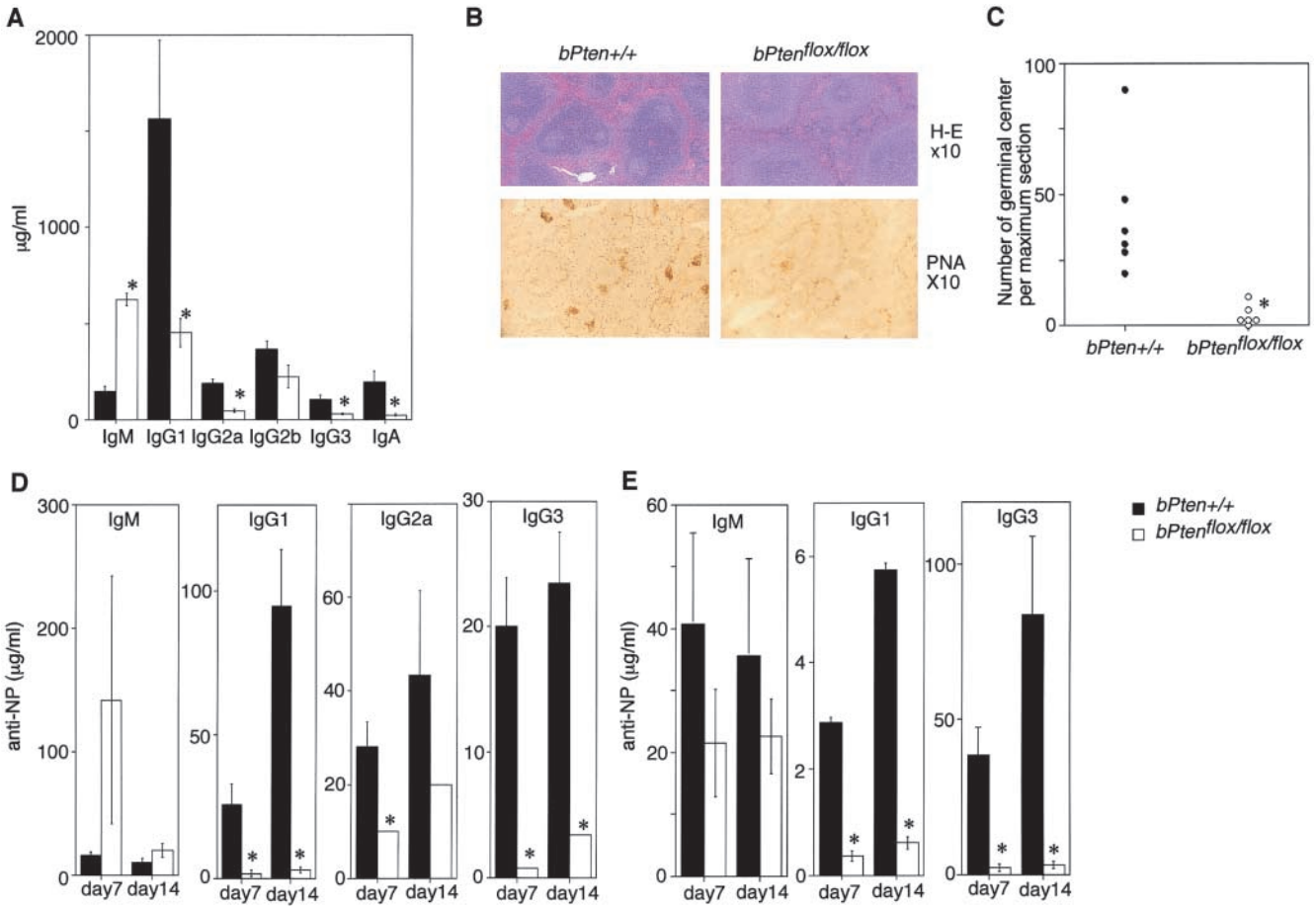

Figure 3. Reduced antigen-specific IgG production and germinal center formation in bPten$^{flox/flox}$ mice. (A) Serum immunoglobulin levels of unimmunized 8-wk-old mice. Serum IgM was increased in *bPten*$^{flox/flox}$ mice while most IgG subclasses and IgA were decreased compared with the WT. (B and C) Germinal center formation. After injection of TD-antigen (NP-CG), the number of germinal centers was markedly reduced in *bPten*$^{flox/flox}$ mice as determined by H&E staining (B, top panel); PNA staining (B, bottom panel); and total counts (C). For C, the total number of germinal centers per spleen section was plotted. Magnification in B, ×10. (D) Production of TD antigen-specific IgGs. Serum levels of specific IgGs induced by injection of NP-CG were significantly decreased in *bPten*$^{flox/flox}$ mice. (E) Production of TI antigen-specific Igs. Serum levels of specific IgGs induced by injection of TI antigen (NP-Ficoll) were also strikingly diminished in *bPten*$^{flox/flox}$ mice. Results are expressed as the mean ± SEM for six mice per group.

the addition of IL-4. These aspects of isotype switching were reduced in *bPten*$^{flox/flox}$ B cells, a result confirmed by ELISA analysis of culture supernatants (Fig. 4 B).

Isotype switching depends on transcription of class-specific mRNAs in which the Iμ exon is spliced onto the 5′ exon of another C_H gene (28). Specific immunoglobulin transcripts can be identified by RT-PCR using primers specific for each C_H gene (29). We stimulated *bPten*$^{flox/flox}$ spleen cells with LPS plus IL-4 and observed that, while transcription of germline transcripts was intact, there was a dramatic reduction in Iμ-Cγ3 and Iμ-Cγ1 post-switch transcripts (Fig. 4 C). These results imply that Pten deficiency leads to a defect in CSR.

CSR depends in part on the activity of AID, a member of the RNA-editing cytidine deaminase family. AID was recently reported to regulate CSR (21) and is activated by LPS in vitro as well as by antigens in vivo. In *bPten*$^{flox/flox}$ mice, AID expression was markedly reduced (Fig. 4 C). In

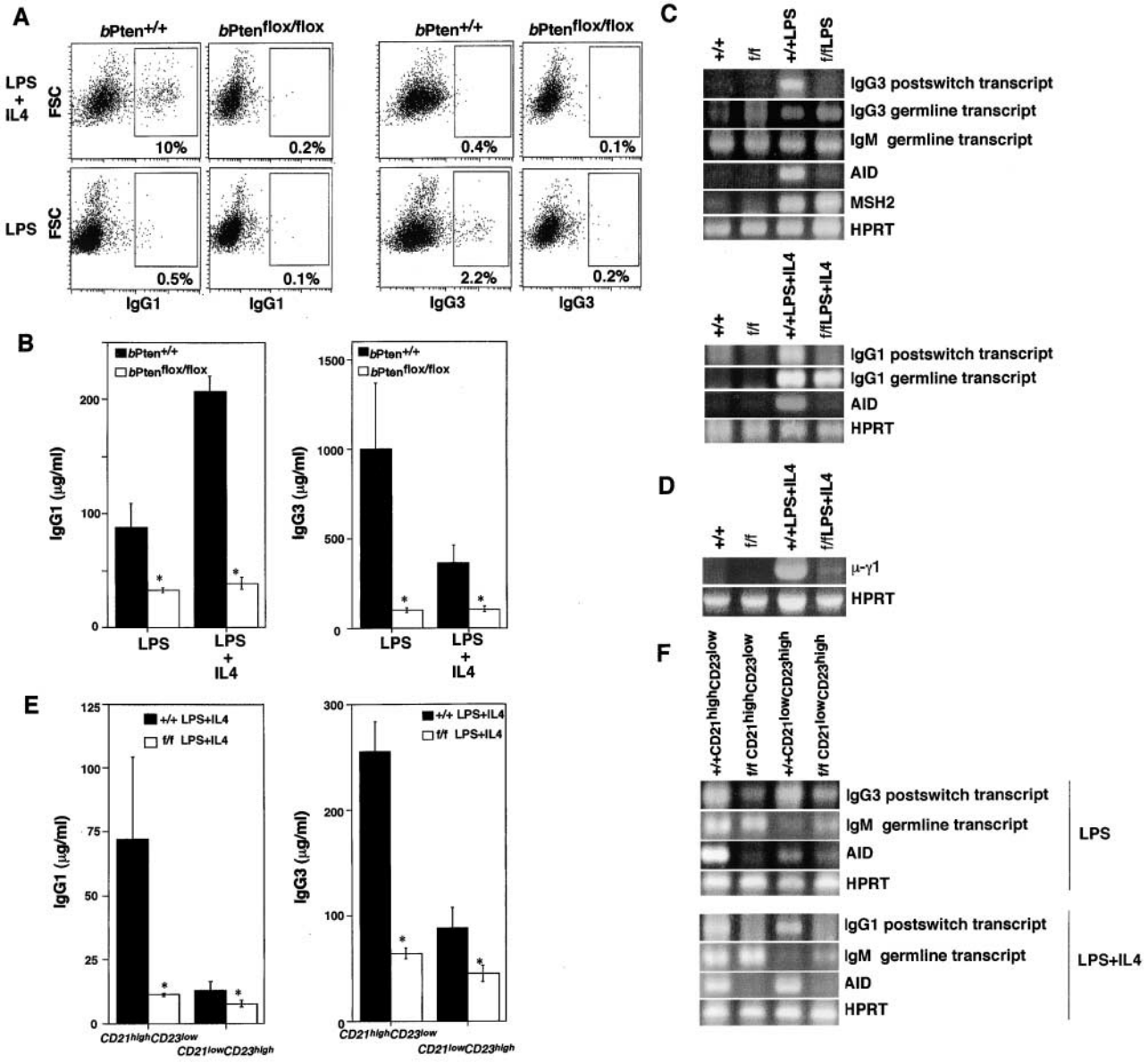

Figure 4. Reduction of CSR associated with impaired induction of AID in Pten-deficient B cells. (A and B) Defect in IgG1 and IgG3 production. B cells from 8-wk-old *bPten*$^{flox/flox}$ and control mice were stimulated with LPS, or LPS plus IL-4, and production of IgG1 and IgG3 on the cell surface (A) and in culture supernatants (B) was analyzed by flow cytometry and ELISA, respectively. For B, results are expressed as the mean ± SEM for three mice per group. (C) Reduction in post-switch transcripts. IgG1 (bottom panel) and IgG3 (top panel) post-switch transcripts were analyzed by RT-PCR. Induction of AID expression was almost absent in *bPten*$^{flox/flox}$ B cells. (D) Impaired switching at the DNA level. μ-γ1 DC-PCR products were profoundly diminished in stimulated mutant B cells. (E and F) CSR in isolated $CD21^{high}CD23^{low}$ (MZB) and $CD21^{low}CD23^{high}$ (FOB) cells. Production of IgG1 and IgG3 postswitch transcripts and AID expression were reduced in both populations of *bPten*$^{flox/flox}$ B cells. Data shown are representative of three independent experiments.

contrast, the expression of MSH2, a mismatch repair gene also important for CSR (30, 31), was not significantly different in *bPten*$^{+/+}$ and *bPten*$^{flox/flox}$ B cells.

To directly examine DNA rearrangement in the Ig locus, we performed digestion-circularization (DC) PCR of DNA obtained from splenic B cells stimulated with LPS plus IL-4. As shown in Fig. 4 D, μ-γ1 DC-PCR products were amplified in DNA from stimulated splenic *bPten*$^{+/+}$ B cells but diminished in DNA from stimulated *bPten*$^{flox/flox}$ B cells. This result demonstrates that Pten deficiency leads to a failure in CSR. To rule out the possibility that the observed defect in CSR was due to differences in the relative numbers of particular cell populations, we examined Ig production and CSR in purified CD21^{high}CD23^{low} (MZB) cells and CD21^{low}CD23^{high} (FOB) cells by ELISA and RT-PCR. Production of IgG1 and IgG3 in response to stimulation with LPS plus IL-4 was impaired in both CD21^{high}CD23^{low} and CD21^{low}CD23^{high} cells of *bPten*$^{flox/flox}$ mice (Fig. 4 E). Similarly, the synthesis of post-switch transcripts and AID expression were reduced equally in *bPten*$^{flox/flox}$ CD21^{high}CD23^{low} and CD21^{low}CD23^{high} cells compared with the WT (Fig. 4 F). These data demonstrate that Pten is indispensable for CSR, presumably because Pten regulates the induction of AID expression.

Autoantibody Secretion. Pten deficiency has been previously associated with autoimmunity (10, 11), and B cell–specific Pten-deficient mice have increased numbers of autoantibody-producing B1 cells (15). We therefore examined serum autoantibody titers of *bPten*$^{flox/flox}$ mice at 6–8 wk and 6–8 mo of age. Both age groups of mutant mice produced significantly greater amounts of anti-ssDNA IgM Ab compared with *bPten*$^{+/+}$ mice in both absolute and relative (% ssDNA/total IgM) terms (Fig. 5). While the absolute amount of anti-ssDNA IgG Ab was not increased significantly in *bPten*$^{flox/flox}$ mice, the relative amount of IgG autoantibody (% ssDNA/total IgG) was elevated. The observed impairment of CSR may partially mitigate the elevation of IgG autoantibodies in *bPten*$^{flox/flox}$ mice.

Resistance to Apoptosis, Enhanced Proliferation, and Increased Migration. We next subjected isolated MZB and FOB populations to various apoptotic, proliferative, and migratory stimuli. "Small dense" *bPten*$^{flox/flox}$ B cells treated in vitro with immobilized anti-IgM were significantly more resistant to apoptosis than *bPten*$^{+/+}$ small dense B cells (Fig. 6 A), suggesting that the increase in MZB cells in *bPten*$^{flox/flox}$ mice might be due at least in part to enhanced resistance to apoptosis.

To examine the proliferation of peripheral B cells, purified splenic CD21^{high}CD23^{low} (MZB) cells and CD21^{low}CD23^{high} (FOB) cells were stimulated in vitro as indicated in Fig. 6 B. Both populations from *bPten*$^{flox/flox}$ mice showed enhanced proliferation compare with the WT in response to stimuli such as anti-IgM, anti-CD40, LPS, or PDBu (phorbol-12, 13-dibutyrate) plus ionomycin. Thus, hyperproliferation contributes to the increased numbers of MZB cells in *bPten*$^{flox/flox}$ mice.

Dammers et al. have reported that MZB cells are derived from a subset of FOB cells by migration (32), although the origin of MZB cells remains controversial. If an absence of Pten enhanced the migration of FOB cells such that more of them became MZB cells, one would expect to see decreased numbers of FOB cells and correspondingly increased numbers of MZB cells, just as we observe in *bPten*$^{flox/flox}$ mice. To test FOB migration, we used transwell migration

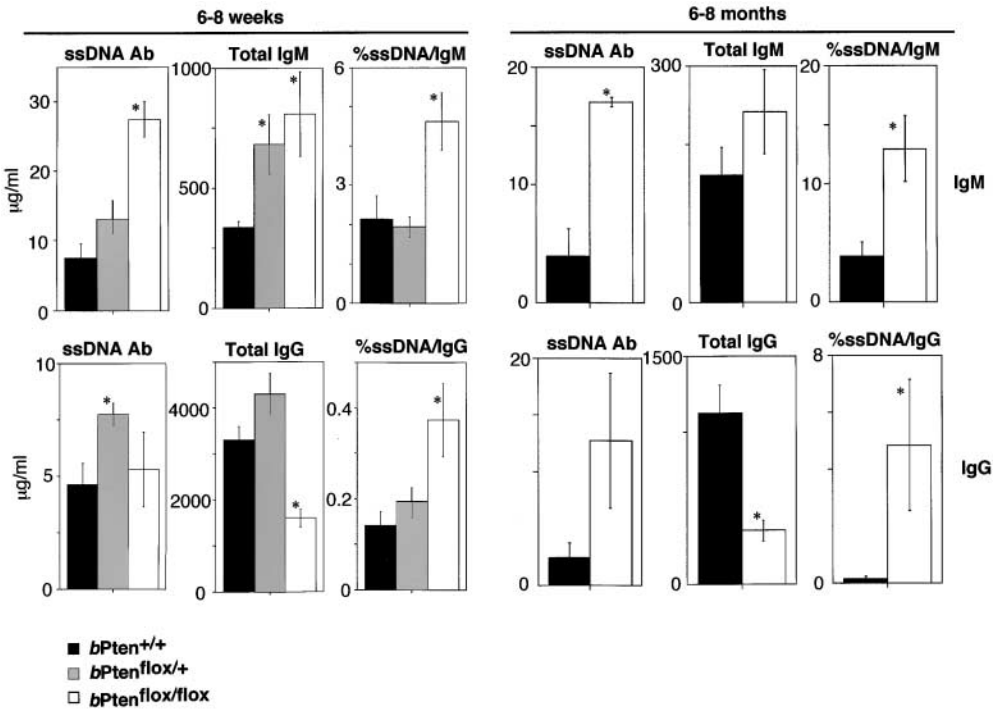

Figure 5. Autoantibody secretion by Pten-deficient B cells. Concentration of serum anti-ssDNA autoantibodies of the IgM class (top panel) and IgG class (bottom panel) in 6–8-wk-old mice (left panel) and 6–8-mo-old mice (right panel) as determined by ELISA. Pten-deficient mice in both age groups produced significantly greater amounts of anti-ssDNA IgM Ab in both absolute and relative (% ssDNA/total IgM) terms. While the absolute amount of anti-ssDNA IgG Ab was not increased in the mutant mice, the relative amount of IgG autoantibody was elevated. Results are expressed as the mean ± SEM for eight mice per group.

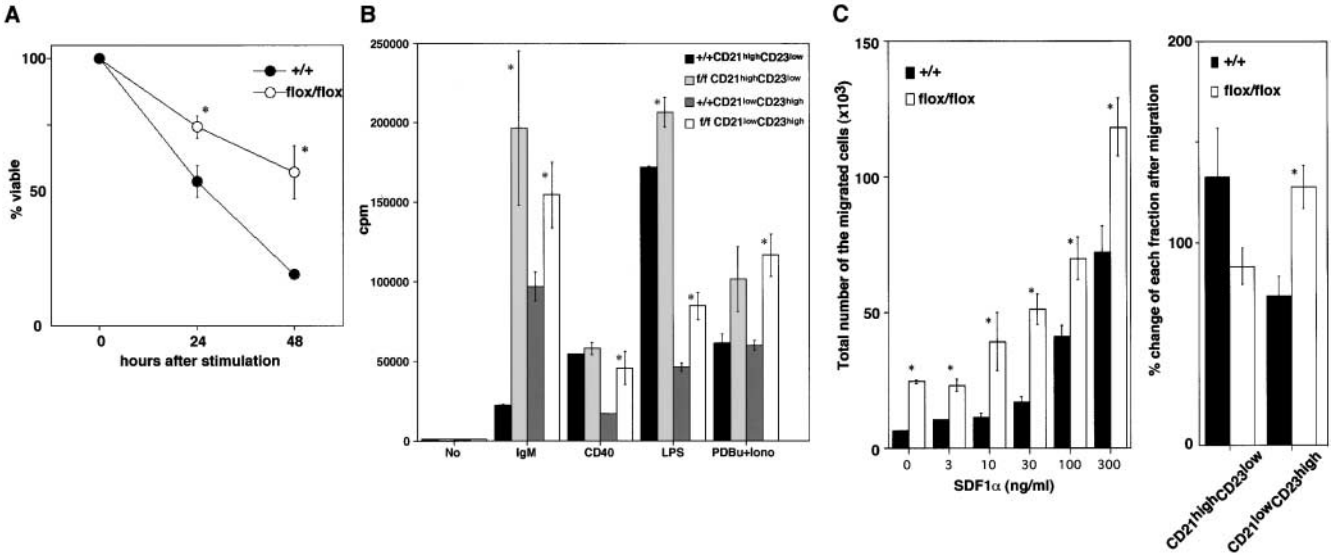

Figure 6. Resistance to apoptosis, enhanced proliferation, and increased migration of Pten-deficient B cells. (A) Resistance to apoptosis. Small dense B cells from 8-wk-old mice were stimulated for 24 h with immobilized anti-IgM (100 μg/ml). Cell viability was determined by trypan blue exclusion. The percentage of viable cells remaining after treatment as compared with the viability of untreated cells cultured for the same length of time is shown. The percentage of viable cells without IgM stimulation: 80 ± 5% (*bPten*$^{+/+}$) and 75 ± 4% (*bPten*$^{flox/flox}$) after 24 h; 48 ± 2% (*bPten*$^{+/+}$) and 56 ± 6% (*bPten*$^{flox/flox}$) after 48 h. Results are expressed as the mean ± SEM for four mice per group. (B) Hyperproliferation. Purified splenic B cells from 6–8-wk-old *bPten*$^{+/+}$ and *bPten*$^{flox/flox}$ mice were incubated with the indicated stimuli and proliferation was measured by thymidine uptake. Both CD21^{high}CD23^{low} (MZB) and CD21^{low}CD23^{high} (FOB) populations from *bPten*$^{flox/flox}$ mice showed enhanced proliferation. Mean thymidine uptake ± SEM for three mice per group is shown. (C) Enhanced migration. Left panel: purified splenic B cells from 6–8-wk-old *bPten*$^{+/+}$ and *bPten*$^{flox/flox}$ mice were assayed for transmigration by culturing them in Transwell culture dish inserts for 3 h in the presence of the indicated concentrations of SDF-1α. The migration of Pten-deficient B cells consistently exceeded that of the control. The mean number of migrated cells ± SEM for three mice per group is shown. Right panel: the % change in MZB and FOB populations before and after migration in the presence of SDF-1α (300 ng/ml). CD21^{high}CD23^{low} cells (MZB) from WT and *bPten*$^{flox/flox}$ mice are both highly mobile, but CD21^{low}CD23^{high} cells (FOB) from Pten-deficient mice are much more mobile than those from the WT. Mean % change ± SEM for three mice per group is shown.

assays to measure the induction of directed cellular migration of purified splenic B cells in a gradient of the chemokine SDF-1α (stromal cell–derived factor-1α). As shown in the left panel of Fig. 6 C, the migration of Pten-deficient B cells was consistently greater than that of controls, even in the absence of SDF-1α.

To clarify which cell population, MZB or FOB, was responsible for the enhanced splenic B cell migration, the percent change in these cell populations before and after migration was calculated (Fig. 6 C). In *bPten*$^{+/+}$mice, CD21^{high}CD23^{low} cells were more mobile than CD21^{low} CD23^{high} cells, consistent with a previous report (33). In contrast, CD21^{low}CD23^{high} cells from *bPten*$^{flox/flox}$ mice were much more mobile than either CD21^{low}CD23^{high} cells or CD21^{high}CD23^{low} cells from *bPten*$^{+/+}$ mice. These data suggest that the reduction in the FOB population in *bPten*$^{flox/flox}$ mice can be attributed to the enhanced migration properties of these cells.

Activation of PKB/Akt. Regulation of PKB/Akt activation by Pten is critical for normal apoptosis in MEF and for proliferation/apoptosis in T cells (7, 11). We therefore analyzed the phosphorylation of PKB/Akt in *bPten*$^{flox/flox}$ splenic B cells. After stimulation with anti-IgM, densitometric analysis showed that phosphorylated PKB/Akt was significantly elevated in *bPten*$^{flox/flox}$ B cells compared with *bPten*$^{+/+}$ B cells (Fig. 7 A). Furthermore, phosphorylation was completely abolished in both *bPten*$^{+/+}$ and *bPten*$^{flox/flox}$ B cells by the addition of an optimal amount of either of the PI3′K inhibitors wortmannin or LY294002. As shown in Fig. 7 B, the abnormal activation of PKB/Akt was observed in both B cell subsets in *bPten*$^{flox/flox}$ spleens. Thus, in both MZB and FOB cells, as in T cells and MEF, PKB/Akt is activated via a PI3′K-mediated pathway that is subject to negative regulation by Pten.

Discussion

To continue our studies of the important tumor suppressor Pten, we have generated and characterized B cell–specific Pten-deficient mice. To our surprise, *bPten*$^{flox/flox}$ mice have shown no signs of B cell malignancies, although most T cell–specific Pten-deficient mice develop T cell lymphomas (11), and Pten mutations occur in human sporadic B cell malignancies (12–14). We have initiated the crossing of *bPten*$^{flox/flox}$ mice into the p53 null genetic background to better assess the onset of B cell malignancy in the absence of Pten.

In this study, *bPten*$^{flox/flox}$ mice showed an increase in MZB cells and a decrease in FOB cells, suggesting that Pten is important for the maintenance of normal B cell subsets in the spleen. It has been proposed that MZB cells may be derived from a subset of FOB cells that migrates

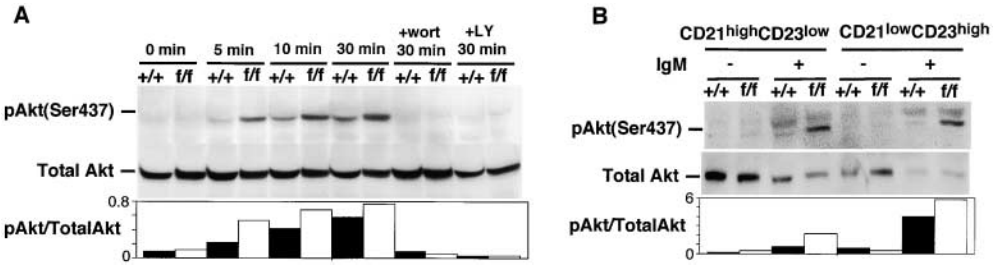

Figure 7. Increased phosphorylation of Akt in Pten-deficient B cells. (A) Top panel: expression of phospho-PKB/Akt in total splenic B cells. Whole cell lysates were prepared from purified splenic B cells of 6–8-wk-old *bPten*$^{+/+}$ and *bPten*$^{flox/flox}$ mice. Cells were stimulated with anti-IgM for the indicated times. A total of 20 μg extract protein was subjected to Western blotting to evaluate the expression of phospho-PKB/Akt (top band) and total PKB/Akt (bottom band; control). Increased phosphorylation of PKB/Akt is evident in extracts of mutant B cells, and this phosphorylation is dependent on PI3′K activation as determined by the addition of the PI3′K inhibitors wortmannin (wort) and LY294002 (LY). Bottom panel: densitometric quantitation of phospho-PKB/Akt levels relative to total cellular PKB/Akt. (B) Top panel: expression of phospho-PKB/Akt in MZB and FOB populations. Increased phosphorylation of PKB/Akt can be seen in Western blot analyses of extracts of isolated CD21^{high}CD23^{low} and CD21^{low}CD23^{high} cells. Bottom panel: densitometric quantitation of phospho-PKB/Akt levels relative to total cellular PKB/Akt. Results shown are representative of three independent experiments.

into an unknown cytokine milieu present outside the follicular zone (32). Knockout studies have shown that Pyk2 (33), Lsc (34), and DOCK2 (35), all molecules involved in cell motility, are indispensable for MZB formation. The reduction in FOB cells observed in the absence of Pten may thus be due to enhanced migration of FOB cells to this region, where they might become MZB cells or otherwise enter into the red pulp. CD21^{high}CD23^{low} B cells also accumulated in *bPten*$^{flox/flox}$ lymph nodes, confirming that Pten-deficient CD21^{high}CD23^{low} B cells have an unusual recirculation pattern similar to that of WT FOB cells. In addition, PKB/Akt activation was increased in both MZB and FOB cells in the absence of Pten. Recently, MZB cells were reported to be decreased in mutant mice lacking p110δ, a subunit of PI3′K (36, 37). Thus, PI3′Kδ may be a key molecule responsible for the generation of abundant MZB cells in *bPten*$^{flox/flox}$ mice. We are in the process of crossing *bPten*$^{flox/flox}$ mice to strains lacking various PI3′K structural and regulatory subunits (36–40) to clarify the contribution of the PI3′K/PIP3 pathway to the generation of MZB cells.

Our data do not formally exclude the possibility that MZB cells are derived from B cells at the transitional, fetal or perinatal stages (41–43). The challenge has been to isolate sufficient numbers of cells from each of these purified subpopulations to test in the transplantation assay. Investigations to this end are ongoing.

Like CD40- and CD40L-deficient mice (44, 45), *bPten*$^{flox/flox}$ mice show reduced germinal center formation associated with impaired B cell activation signaling. Interestingly, these deficits were apparent even in the presence of strong activation signals delivered via IgM and CD40, and even though the activation of intracellular signaling pathways mediated by PKB/Akt and Btk was intact (unpublished data). FOB cells are required to form germinal centers, and the reduction in this cell population in *bPtenf*$^{lox/flox}$ mice may account for the observed defect.

Several lines of evidence in this study indicate that CSR is impaired in *bPten*$^{flox/flox}$ mice. First, MZB and B1 cells are important for TI responses (33, 46), but even though these populations were elevated in *bPten*$^{flox/flox}$ mice, the production of antigen-specific IgG in response to TI-II antigen was profoundly decreased. Second, *bPten*$^{flox/flox}$ MZB and FOB cells showed defective class switching at the cellular level. Third, Ig germline transcripts were intact in *bPten*$^{flox/flox}$ B cells but the expression of AID, an essential factor for CSR, was diminished. Little is presently known about the regulation of AID gene expression and the link between Pten and AID. It may be germane that mice deficient for SHIP, a phosphatase whose substrate is also PIP3, have intact CSR (47). This result implies that the defect in *bPten*$^{flox/flox}$ mice could be PIP3-independent. We are undertaking studies of the transcriptional regulation of the AID gene to address how Pten might directly or indirectly influence its expression.

MZB cells are presumed to have a critical role in host defense against bacterial pathogens (16, 17). However, in preliminary experiments, no differences were observed between *bPten*$^{+/+}$ *and bPten*$^{flox/flox}$ mice subjected to lethal *Staphylococcus aureus* infections. It is possible that, even though they have greater numbers of the anti-bacterial MZB cells, the CSR defect in *bPten*$^{flox/flox}$ B cells leads to inadequate host defense.

bPten$^{flox/flox}$ mice display marked elevations in B1 cell numbers and serum levels of autoantibodies, particularly those of the IgM isotype. These B1 cells were CD21^{-} and CD23^{-} (unpublished data), suggesting that the increase in the CD21^{-}CD23^{-} population in the mutant mice was due to an increase in B1 cells. Peritoneal B1 cells are involved in the production of autoreactive antibodies (15) and may constitute up to 40% of the total IgA-secreting plasma cell population (48). *bPten*$^{flox/flox}$ mice showed reduced serum IgA and normal titers of IgG autoantibodies in spite of their increased B1 cells. This phenotype is consistent with the impaired CSR in Pten-deficient B1 cells. The increase in the B1 population may be due to the abnormal activation of the PI3′K/PIP3/Akt pathway in *bPten*$^{flox/flox}$ mice. Mice deficient for either the p85α or p110δ subunit of PI3′K show a marked reduction in B1 cells (36–39). Our planned analyses of p85α$^{-/-}$; *bPten*$^{flox/flox}$ and p110δ$^{-/-}$; *bPten*$^{flox/flox}$ mice should further define the role of the PI3′K/PIP3/Akt pathway and its regulation by Pten in B1 cell generation

and autoantibody secretion. Curiously, despite elevated levels of autoantibodies, our *bPten*$^{flox/flox}$ mice have survived for over a year without showing definite histological abnormalities characteristic of autoimmune disease. This result stands in contrast to the development of autoimmune disorders in mice heterozygous for the null Pten mutation (10) and in T cell–specific Pten-deficient mice (11). Impaired CSR may derail the onset of autoimmune disease in *bPten*$^{flox/flox}$ mice.

In conclusion, we have demonstrated that Pten deficiency alters B1, MZB, and FOB B cell subsets in mice. Moreover, Pten deficiency causes an impairment of immunoglobulin isotype switching. Pten is thus an important regulator of B cell development and homeostasis in the immune system.

We would like to thank Dr. Robert C. Rickert, Dr. Werner Müller, and Dr. Klaus Rajewsky (University of Cologne) for providing the CD19Cre transgenic mice; Dr. Tetsuo Noda (Tohoku University), Dr. Manabu Fukumoto (Tohoku University), Dr. Yasuhisa Hokazono and Dr. Yuichi Aiba (Tokyo Medical and Dental University), Dr. Eiko Sakai and Ms. Nana Iwami (Osaka University) for technical assistance and helpful discussions; Dr. Anna Cumuno (Ontario Cancer Institute) and Dr. Tomohiro Kurosaki (Kansai Medical University) for critically reading the manuscript; Dr. Mary Saunders for scientific editing; and Ms. Miki Sato Suzuki for her valuable assistance.

This work was supported by grants from the Ministry of Education, Science, Sports and Culture (Japan), the Osaka Cancer Research Society, the Novartis Foundation (Japan) for the Promotion of Science, the Naito Foundation, the ONO Medical Research Foundation, and the Sumitomo Foundation.

Submitted: 1 July 2002
Revised: 7 January 2003
Accepted: 22 January 2003

References

1. Li, J., C. Yen, D. Liaw, K. Podsypanina, S. Bose, S.I. Wang, J. Puc, C. Miliaresis, L. Rodgers, R. McCombie, et al. 1997. PTEN, a putative protein tyrosine phosphatase gene mutated in human brain, breast, and prostate cancer. *Science*. 275: 1943–1947.
2. Liaw, D., D.J. Marsh, J. Li, P.L. Dahia, S.I. Wang, Z. Zheng, S. Bose, K.M. Call, H.C. Tsou, M. Peacocke, et al. 1997. Germline mutations of the PTEN gene in Cowden disease, an inherited breast and thyroid cancer syndrome. *Nat. Genet.* 16:64–67.
3. Marsh, D.J., P.L. Dahia, Z. Zheng, D. Liaw, R. Parsons, R.J. Gorlin, and C. Eng. 1997. Germline mutations in PTEN are present in Bannayan-Zonana syndrome. *Nat. Genet.* 16:333–334.
4. Myers, M.P., and N.K. Tonks. 1997. PTEN: sometimes taking it off can be better than putting it on. *Am. J. Hum. Genet.* 61:1234–1238.
5. Maehama, T., and J.E. Dixon. 1998. The tumor suppressor, PTEN/MMAC1, dephosphorylates the lipid second messenger, phosphatidylinositol 3,4,5-trisphosphate. *J. Biol. Chem.* 273:13375–13378.
6. Suzuki, A., J.L. de la Pompa, V. Stambolic, A.J. Elia, T. Sasaki, I. del Barco Barrantes, A. Ho, A. Wakeham, A. Itie, W. Khoo, et al. 1998. High cancer susceptibility and embryonic lethality associated with mutation of the PTEN tumor suppressor gene in mice. *Curr. Biol.* 8:1169–1178.
7. Stambolic, V., A. Suzuki, J.L. de la Pompa, G.M. Brothers, C. Mirtsos, T. Sasaki, J. Ruland, J.M. Penninger, D.P. Siderovski, and T.W. Mak. 1998. Negative regulation of PKB/Akt-dependent cell survival by the tumor suppressor PTEN. *Cell.* 95:29–39.
8. Stambolic, V., M.S. Tsao, D. Macpherson, A. Suzuki, W.B. Chapman, and T.W. Mak. 2000. High incidence of breast and endometrial neoplasia resembling human Cowden syndrome in pten+/− mice. *Cancer Res.* 60:3605–3611.
9. Podsypanina, K., L.H. Ellenson, A. Nemes, J. Gu, M. Tamura, K.M. Yamada, C. Cordon-Cardo, G. Catoretti, P.E. Fisher, and R. Parsons. 1999. Mutation of Pten/Mmac1 in mice causes neoplasia in multiple organ systems. *Proc. Natl. Acad. Sci. USA.* 96:1563–1568.
10. Di Cristofano, A., P. Kotsi, Y.F. Peng, C. Cordon-Cardo, K.B. Elkon, and P.P. Pandolfi. 1999. Impaired Fas response and autoimmunity in Pten+/− mice. *Science.* 285:2122–2125.
11. Suzuki, A., M.T. Yamaguchi, T. Ohteki, T. Sasaki, T. Kaisho, Y. Kimura, R. Yoshida, A. Wakeham, T. Higuchi, M. Fukumoto, et al. 2001. T cell-specific loss of Pten leads to defects in central and peripheral tolerance. *Immunity.* 14:523–534.
12. Gronbaek, K., J. Zeuthen, P. Guldberg, E. Ralfkiaer, and K. Hou-Jensen. 1998. Alterations of the MMAC1/PTEN gene in lymphoid malignancies. *Blood.* 91:4388–4390.
13. Nakahara, Y., H. Nagai, T. Kinoshita, T. Uchida, S. Hatano, T. Murate, and H. Saito. 1998. Mutational analysis of the PTEN/MMAC1 gene in non-Hodgkin's lymphoma. *Leukemia.* 12:1277–1280.
14. Hyun, T., A. Yam, S. Pece, X. Xie, J. Zhang, T. Miki, J.S. Gutkind, and W. Li. 2000. Loss of PTEN expression leading to high Akt activation in human multiple myelomas. *Blood.* 96:3560–3568.
15. Murakami, M., T. Tsubata, M. Okamoto, A. Shimizu, S. Kumagai, H. Imura, and T. Honjo. 1992. Antigen-induced apoptotic death of Ly-1 B cells responsible for autoimmune disease in transgenic mice. *Nature.* 357:77–80.
16. Cyster, J.G. 2000. B cells on the front line. *Nat. Immunol.* 1:9–10.
17. Kraal, G. 1992. Cells in the marginal zone of the spleen. *Int. Rev. Cytol.* 132:31–74.
18. Oliver, A.M., F. Martin, and J.F. Kearney. 1999. IgM highCD21high lymphocytes enriched in the splenic marginal zone generate effector cells more rapidly than the bulk of follicular B cells. *J. Immunol.* 162:7198–7207.
19. Kumararatne, D.S., H. Bazin, and I.C. MacLennan. 1981. Marginal zones: the major B cell compartment of rat spleens. *Eur. J. Immunol.* 11:858–864.
20. Oliver, A.M., F. Martin, G.L. Gartland, R.H. Carter, and J.F. Kearney. 1997. Marginal zone B cells exhibit unique activation, proliferative and immunoglobulin secretory responses. *Eur. J. Immunol.* 27:2366–2374.
21. Muramatsu, M., K. Kinoshita, S. Fagarasan, S. Yamada, Y. Shinkai, and T. Honjo. 2000. Class switch recombination and hypermutation require activation-induced cytidine deaminase (AID), a potential RNA editing enzyme. *Cell.* 102:553–563.
22. Rickert, R.C., J. Roes, and K. Rajewsky. 1997. B lymphocyte-specific, Cre-mediated mutagenesis in mice. *Nucleic Ac-*

ids Res. 25:1317–1318.
23. Kaisho, T., F. Schwenk, and K. Rajewsky. 1997. The roles of gamma 1 heavy chain membrane expression and cytoplasmic tail in IgG1 responses. *Science.* 276:412–415.
24. Satoh, M., A. Kumar, Y.S. Kanwar, and W.H. Reeves. 1995. Anti-nuclear antibody production and immune-complex glomerulonephritis in BALB/c mice treated with pristane. *Proc. Natl. Acad. Sci. USA.* 92:10934–10938.
25. Chu, C.C., W.E. Paul, and E.E. Max. 1992. Quantitation of immunoglobulin mu-gamma 1 heavy chain switch region recombination by a digestion-circularization polymerase chain reaction method. *Proc. Natl. Acad. Sci. USA.* 89:6978–6982.
26. Stall, A.M., S. Adams, L.A. Herzenberg, and A.B. Kantor. 1992. Characteristics and development of the murine B-1b (Ly-1 B sister) cell population. *Ann. N. Y. Acad. Sci.* 651:33–43.
27. Marcos, M.A., F. Huetz, P. Pereira, J.L. Andreu, A.C. Martinez, and A. Coutinho. 1989. Further evidence for coelomic-associated B lymphocytes. *Eur. J. Immunol.* 19:2031–2035.
28. Esser, C., and A. Radbruch. 1990. Immunoglobulin class switching: molecular and cellular analysis. *Annu. Rev. Immunol.* 8:717–735.
29. Li, S.C., P.B. Rothman, J. Zhang, C. Chan, D. Hirsh, and F.W. Alt. 1994. Expression of I mu-C gamma hybrid germline transcripts subsequent to immunoglobulin heavy chain class switching. *Int. Immunol.* 6:491–497.
30. Ehrenstein, M.R., and M.S. Neuberger. 1999. Deficiency in Msh2 affects the efficiency and local sequence specificity of immunoglobulin class-switch recombination: parallels with somatic hypermutation. *EMBO J.* 18:3484–3490.
31. Schrader, C.E., W. Edelmann, R. Kucherlapati, and J. Stavnezer. 1999. Reduced isotype switching in splenic B cells from mice deficient in mismatch repair enzymes. *J. Exp. Med.* 190:323–330.
32. Dammers, P.M., N.K. de Boer, G.J. Deenen, P. Nieuwenhuis, and F.G. Kroese. 1999. The origin of marginal zone B cells in the rat. *Eur. J. Immunol.* 29:1522–1531.
33. Guinamard, R., M. Okigaki, J. Schlessinger, and J.V. Ravetch. 2000. Absence of marginal zone B cells in Pyk-2-deficient mice defines their role in the humoral response. *Nat. Immunol.* 1:31–36.
34. Girkontaite, I., K. Missy, V. Sakk, A. Harenberg, K. Tedford, T. Potzel, K. Pfeffer, and K.D. Fischer. 2001. Lsc is required for marginal zone B cells, regulation of lymphocyte motility and immune responses. *Nat. Immunol.* 2:855–862.
35. Fukui, Y., O. Hashimoto, T. Sanui, T. Oono, H. Koga, M. Abe, A. Inayoshi, M. Noda, M. Oike, T. Shirai, and T. Sasazuki. 2001. Haematopoietic cell-specific CDM family protein DOCK2 is essential for lymphocyte migration. *Nature.* 412:826–883.
36. Okkenhaug, K., A. Bilancio, G. Farjot, H. Priddle, S. Sancho, E. Peskett, W. Pearce, S.E. Meek, A. Salpekar, M.D. Waterfield, et al. 2002. Impaired B and T cell antigen receptor signaling in p110delta PI 3-kinase mutant mice. *Science.* 297:1031–1034.
37. Clayton, E., G. Bardi, S.E. Bell, D. Chantry, C.P. Downes, A. Gray, L.A. Humphries, D. Rawlings, H. Reynolds, E. Vigorito, and M. Turner. 2002. A crucial role for the p110delta subunit of phosphatidylinositol 3-kinase in B cell development and activation. *J. Exp. Med.* 196:753–763.
38. Fruman, D.A., S.B. Snapper, C.M. Yballe, L. Davidson, J.Y. Yu, F.W. Alt, and L.C. Cantley. 1999. Impaired B cell development and proliferation in absence of Phosphoinositide 3-kinase p85alpha. *Science.* 283:393–397.
39. Suzuki, H., Y. Terauchi, M. Fujiwara, S. Aizawa, Y. Yazaki, T. Kadowaki, and S. Koyasu. 1999. Xid-like immunodeficiency in mice with disruption of the p85alpha subunit of phosphoinositide 3-kinase. *Science.* 283:390–392.
40. Sasaki, T., J. Irie-Sasaki, R.G. Jones, A.J. Oliveira-dos-Santos, W.L. Stanford, B. Bolon, A. Wakeham, A. Itie, D. Bouchard, I. Kozieradzki, et al. 2000. Function of PI3Kgamma in thymocyte development, T cell activation, and neutrophil migration. *Science.* 287:1040–1046.
41. Martin, F., A.M. Oliver, and J.F. Kearney. 2001. Marginal zone and B1 B cells unite in the early response against T-independent blood-borne particulate antigens. *Immunity.* 14:617–629.
42. Carvalho, T.L., T. Mota-Santos, A. Cumano, J. Demengeot, and P. Vieira. 2001. Arrested B lymphopoiesis and persistence of activated B cells in adult interleukin 7(−/−) mice. *J. Exp. Med.* 194:1141–1150.
43. Hao, Z., and K. Rajewsky. 2001. Homeostasis of peripheral B cells in the absence of B cell influx from the bone marrow. *J. Exp. Med.* 194:1151–1164.
44. Xu, J., T.M. Foy, J.D. Laman, E.A. Elliott, J.J. Dunn, T.J. Waldschmidt, J. Elsemore, R.J. Noelle, and R.A. Flavell. 1994. Mice deficient for the CD40 ligand. *Immunity.* 1:423–431.
45. Kawabe, T., T. Naka, K. Yoshida, T. Tanaka, H. Fujiwara, S. Suematsu, N. Yoshida, T. Kishimoto, and H. Kikutani. 1994. The immune responses in CD40-deficient mice: impaired immunoglobulin class switching and germinal center formation. *Immunity.* 1:167–178.
46. Fagarasan, S., and T. Honjo. 2000. T-Independent immune response: new aspects of B cell biology. *Science.* 290:89–92.
47. Liu, Q., T. Sasaki, I. Kozieradzki, A. Wakeham, A. Itie, D.J. Dumont, and J.M. Penninger. 1999. SHIP is a negative regulator of growth factor receptor-mediated PKB/Akt activation and myeloid cell survival. *Genes Dev.* 13:786–791.
48. Kroese, F.G., E.C. Butcher, A.M. Stall, P.A. Lalor, S. Adams, and L.A. Herzenberg. 1989. Many of the IgA producing plasma cells in murine gut are derived from self-replenishing precursors in the peritoneal cavity. *Int. Immunol.* 1:75–84.